A SIMULATED STUDY ON THE PERFORMANCE OF DIESEL ENGINE WITH ETHANOL-DIESEL BLEND FUEL

by

Zhi-Qiang ZHANG [a*], Fu-Quan ZHAO [a,b], Jun DENG [a], and Li-Guang LI [a]

[a] School of Automotive Studies, Tongji University, Shanghai, China
[b] Automobile Engineering Institute, Zhejiang Geely Holding Group Co., LTD, Hangzhou, China

Original scientific paper
DOI: 10.2298/TSCI110630105Z

This paper describes the simulated study on atomization, wall-film formation, combustion and emission forming process of ethanol-diesel blend fuels in a high speed light duty diesel engine. The result shows that increased ethanol volume percentage of the blend fuels could improve atomization and reduce wall-film formation. However, in the meanwhile, with the increased ethanol volume percentage, low heat values of blend fuels decrease, while both total heat releases and cylinder pressures drop. By adding codes into the FIRE software, the NO_x and soot formation region mass fractions are outputted. The simulated results display a good correlation with the NO_x and soot formation. Besides, the NO_x, soot and CO emissions decrease with the increased ethanol volume percentage. The power output of engine penalize, while energy utilization of blend fuels improve and combustion noise reduce, owing to the increased ethanol volume percentage.

Key words: *ethanol-diesel blend fuels, wall-film, NO_x and soot formation region mass fraction, combustion, emissions*

Introduction

With the advantage of lower CO_2 emissions and fuel consumption, diesel engines have been applied more widely in commercial and passenger vehicles. Due to the more stringent emission regulation and the more impended energy crisis, the development of cleaner diesel engines has been conducted by various engine-related techniques, such as exhaust gas re-circulation, multiple injection strategies [1], selective catalytic reduction [2] and diesel particulate filter [3] .

In order to reduce the pollutant emissions and decrease the dependence of the fossil fuels, the fuel-related techniques have been highlighted among many other techniques, such as application of alternative fuels [4, 5], which are friendly to the environment and fulfill wasted oil reclamation. As one kind of renewable alternative fuels, ethanol could be produced by alcoholic fermentation of sugar from vegetable materials, such as corn, sugar cane, sugar beets, or agricultural residues [4]. In addition, owing to its high concentration of the oxygen, ethanol has an advantage of reducing soot emissions. There are many utilizations of ethanol in diesel engine [6, 7], and the most convenient method of employing ethanol in the diesel engine is blending ethanol and diesel with a solubilizer to form uniform and stability blend fuels.

Most combustion of the diesel engine is the diffusion combustion. The combustion and exhaust formation occur at the same time when fuels are injected into the cylinder, atomized and entrained with the air. But a part of the injected fuels are likely to be deposited as a form of

* Corresponding author; e-mail: zhiqiangbucy@126.com

thin liquid wall-film in the combustion chamber, due to incomplete evaporation and spray-wall impinging. Moreover, the undesired storage of wall-film could cause penalty of engine performance and increased exhaust emissions. Many experiments and simulations have been conducted to understand the characteristics of the wall-film formation [8-10].

Comparison between diesel and ethanol-diesel blend fuels indicates that there are some discrepancies of the properties between these kinds of fuels, which could affect the fuel atomization and wall-film forming processes. The main objective of the present paper is to study the effects on fuel atomization and wall-film formation of the ethanol-diesel blend fuels in a high speed light duty diesel engine. Moreover the combustion and exhaust emissions formation are also analyzed. By coupling the codes into the FIRE software to output the NO_x and soot formation region mass fractions, the analysis of the NO_x and soot formation is also further developed.

Simulated model, validation, and properties of ethanol-diesel blend fuels

Simulated model

Model set-up. The mechanism of the simulated gas flow is based on the transport function of mass, momentum and energy conservation. The *k-ζ-f* turbulent model is employed to consider the effect of turbulent on the gas flow, which is based on Durbin's elliptic relaxation concept [11, 12]. Although the calculation time is 15% more than *k-ε* model, the *k-ζ-f* model is more robust, more stable and less sensitive to non-uniformity and clustering of the computational grid [13]. Another novelty of the model is the application of a quasi-linear pressure – strain model in the equation – *f* [14, 15].

The Wave breakup model is employed to simulate the spray breakup process. It should be noted that the initial diameter of droplets should not exceed the value range of the nozzle diameter [16].

For that there are two compositions (ethanol and diesel) existing in the blend fuels, the multi-component evaporation model is chosen, which has been extended by Brenn *et al*. [17].

The Extended coherent flame-3Z model (ECFM-3Z model) is employed to simulate the ethanol-diesel blend fuels' combustion process, which is based on a flame surface density transport function and a mixing model. The ECFM-3Z model can describe inhomogeneous turbulent premixed and diffusion combustion [18]. There are three regions defining in the model which are air, mixture and combustion region. This hypothesis could reflect the essential of the diesel combustion process. And there is a 2-step chemistry mechanism in the ECFM-3Z model, which is listed as follow:

$$C_nH_mO_k + \left(n + \frac{m}{4} - \frac{k}{2}\right)O_2 \rightarrow nCO_2 + \frac{m}{2}H_2O \tag{1}$$

$$C_nH_mO_k + \left(\frac{n}{2} - \frac{k}{2}\right)O_2 \rightarrow nCO + \frac{m}{2}H_2 \tag{2}$$

The NO_x formation obeys the Zeldovich mechanism [19], which contains the following three reactions:

$$N_2 + O \leftrightarrow NO + N \tag{3}$$

$$N + O_2 \leftrightarrow NO + O \tag{4}$$

$$N + OH \leftrightarrow NO + H \tag{5}$$

The soot formation and oxidation model is employed the Kennedy-Hiroyasu--Magnussen model, which combines the chemical and physical reaction to simulate soot's nucleation, surface growth, and oxidation. The processes of particle formation and surface growth are taken to be related functions of the local fuel and soot nuclei concentration, and the predominated flame temperature governing the Arrhenius rate coefficient of the particle mass addition term [20, 21]:

$$S = S_n + S_g + S_o \tag{6}$$

where S is the soot, S_n – the nucleation source, S_g – the surface growth source, S_o – the oxidation soot.

Wall-film model. When the fuel droplets impinging on the combustion chamber, they can stick to the wall, spread and splash to build the wall-film, or reflect to combustion chamber. The possibility of the impinging droplets depends on the major factors, such as wall temperature and droplet Weber number [22].

The wall-film model is based on systematic empirical investigations which have been conducted by Mundo *et al*. [23, 24]. The test matrix of the experiments involved different droplet diameters (60 ~ 150 μm), impact velocities(12 ~ 18 m/s) and impingement angles(4 ~ 65°) as well as smooth and rough walls.

The K-value is a characteristic quantity to distinguish between different impingement regions. Additionally, the K-value is defined as:

$$K = \mathrm{Oh}\,\mathrm{Re}_D^{1.25} = \frac{\rho^{0.75} d_0^{0.75} u_{\perp 0}^{1.25}}{\mu^{0.25}\sigma^{0.5}} \tag{7}$$

where Oh and Re_D are adopted from:

$$\mathrm{Oh} = \frac{\mu}{\sqrt{\rho\sigma d_0}} \tag{8}$$

$$\mathrm{Re}_D = \frac{\rho d_0 u_{\perp 0}}{\mu} \tag{9}$$

The Reynolds number represents the ratio of the fluid micro inertial force and the cohesive force, while the Ohnesorge number is the ratio of the viscous forces and surface tension. ρ is the density, d_0 – the droplet diameter, and $u_{\perp 0}$ – velocity, normal to the wall component of initial droplet μ and σ are the viscosity and surface tension of the droplet.

If the K-value is smaller than 57.7, the droplets could be deposited completely on the wall without rebound or breakup. In the region where $K > 57.7$, with the increased droplet impact momentum, a larger mass percentage is atomized and reflected. During this splashing, the droplets are partially shattered to produce a different droplet size spectrum for the reflected droplets. With the increased K-value, the reflected droplets tend to be smaller.

Simulated condition

The simulated study is conducted for a high speed and light duty diesel engine. The main parameters of the diesel engine are listed in tab. 1.

Considering the combustion chamber is axisymmetric and the number of nozzle holes is eight, the simulated mesh is one eighth of the combustion chamber in order to shorten time. Figure 1 shows the mesh on the top dead center. The protrusion part on the edge of the sidewall is compensation volume, which ensures that the mesh maintains the same compress ratio at any crank angle [25, 26]. Boundary conditions are consistent with the experiments. The tempera-

Table.1 Parameters of the diesel engine

Cylinder diameter × stroke [mm]	85 × 88.1
Connecting nod [mm]	149
Compression ratio	16.2
Number of cylinders	4
Number of nozzle holes	8
Maximum torque [Nm at rpm]	300 at 1800~2800
Rated power [kW at rpm]	100 at 4000
Swirl ratio	1.7

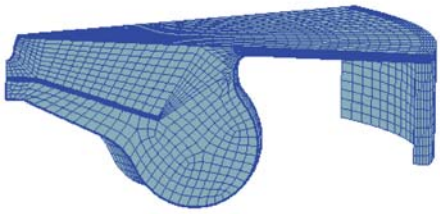

Figure 1. Mesh of the simulation model on the top dead center

tures of the head and surface of the piston are set as 570 K, while the temperature for sidewall of the cylinder is set as 470 K. The range of simulation is from intake valve close time (213° CA) to exhaust valve open time (499° CA).

The speed of simulated studies is 2200 rpm. And the injection strategy is the double injections – pilot and main injections (shown in fig. 2), of which the injection mass are 3 mg and 52 mg per stroke. The concentration of ethanol in the simulation is 97%. The ethanol-diesel blend fuels are injected into combustion chamber through a single nozzle. The ethanol volume percentages of the ethanol-diesel blend fuels are 0%, 10%, 20%, and 30%, abbreviation in ED0, ED10, ED20, and ED30 (ED means the ethanol-diesel blend fuel, while the number means the ethanol volume percentage).

Validation of the simulated model

In order to validate the simulated model, the comparison of the simulated cylinder pressure and NO_x and soot emissions with the experiment are reported in figs. 2 and 3, in which the fuels are diesel. The experimental results are only acquired from the fourth cylinder, of which the intake and exhaust pipes are independent from the other three cylinders in order to avoid the effects of the other cylinders on the results. The experimental and simulated conditions are at 2200 rpm with the same injection strategy (3 mg for pilot injection, 52 mg for main injection), as well as the same intake pressure (0.13 MPa) and temperature (318 K). The cylinder pressure is acquired by the Kistler 6052,

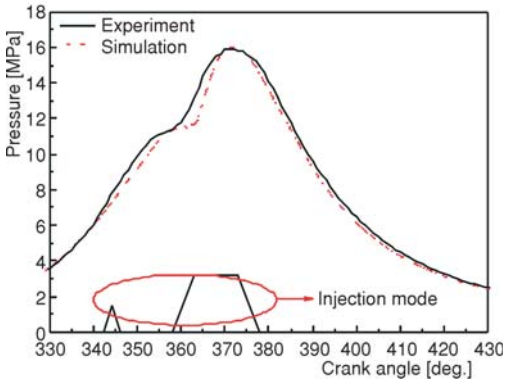

Figure 2. Comparison of the experiment and simulation on cylinder pressure

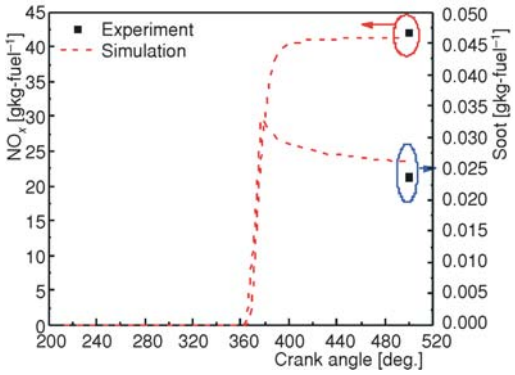

Figure 3. Comparison of the experiment and simulation on NO_x and soot emissions

which is the mean pressure of a set of one hundred work cycles. The NO_x and soot emissions are measured by the AVL CEBII and the AVL 415S smoke meter. Formulas of converting ppm and FSN to g/kg-fuel are consistent with the definition in ref. [27].

Due to the limitation of the simulated models (especially for the 2-step chemistry mechanism of the ECFM-3Z model), there are a few discrepancies of the cylinder pressure around the 342° CA and 358° CA. The discrepancies are not critical to understand the blend fuels' characteristics. The NO_x and soot emissions of the simulation are closed to the experimental results. The simulated results show quite good agreement with the experiment. So the simulated model is validated and suitable for the studies.

Properties of ethanol-diesel blend fuels

The ethanol and diesel could not dissolve together for that the molecular structures of ethanol and diesel are polarity and non-polarity. The properties of ethanol and diesel are listed in the tab. 2. According to the principle of the dissolution in the similar material structure, the heptanol is chosen as the solubilizer for the ethanol-diesel blend fuels, of which the molecular structure includes polarity and non-polarity parts. In all the ethanol-diesel blend fuels, the volume percentage of heptanol is constant as 2%.

Table 2. Properties of diesel and ethanol

Fuel	Sulfur content [ppm]	Cetane number	Flash point [°C]	Low heat value [kJkg^{-1}]	Latent heat of vaporization [kJkg^{-1}]	Ignition limits [%]	Air fuel ratio
Hu.IV 0# Diesel	50	>51	55	42.6	301	1.5~7.6	14.3
Ethanol	–	8	13.5	26.77	904	4.3~19	9.0

Density, viscosity, and surface tension of the ethanol-diesel blend fuels are measured by the MDY-1 type electronic densimeter, NDJ-1S digital viscometer and QBZY-1 automatic surface tension-meter respectively. As reported in figs. 4, 5, and 6, the density, viscosity and surface tension of the ethanol-diesel fuels are decreased with the increased ethanol volume percentage.

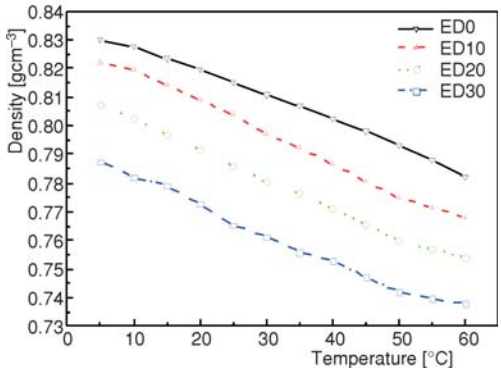

Figure 4. Density of ethanol-diesel fuels

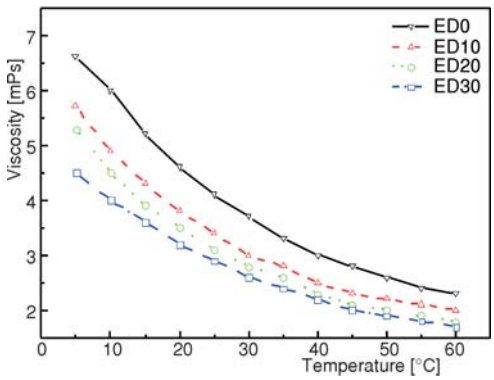

Figure 5. Viscosity of ethanol-diesel fuels

In order to consider the effect of ethanol-diesel fuels on K-values, here define K' as:

$$K' = \frac{\rho^{0.75}}{\mu^{0.25}\sigma^{0.5}} \tag{10}$$

The K' of ethanol-diesel fuels is reported in fig. 7, which is increased with the increased ethanol volume percentage. It implies that the fuels could be more atomized and less deposited, according to the principle of the wall-film model.

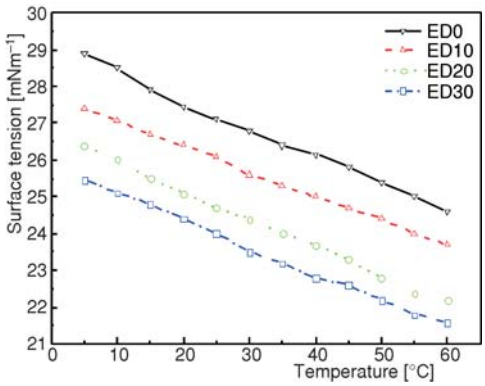

Figure 6. Surface tension of ethanol-diesel fuels

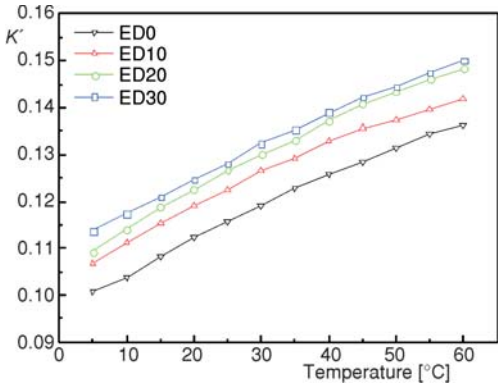

Figure 7. K' of ethanol-diesel fuels

Results and discussion

Effects of ethanol volume percentage on the fuel atomization and wall-film formation

As reported in fig. 2, there are double injections – pilot and main injections. The evaporated fuel mass fractions are almost the same for diesel and blend fuels in the pilot injection period, for the reason that the mass of the injected fuels is just 3 mg. Huge amount of fuels are injected in the main injection, of which the mass is 52 mg. As shown in figs. 8 and 9, due to the reason that the good volatility of ethanol accelerates the evaporation process, the evaporated fuel mass fractions increase while the impinging fuel masses decrease with the increased ethanol volume percentage.

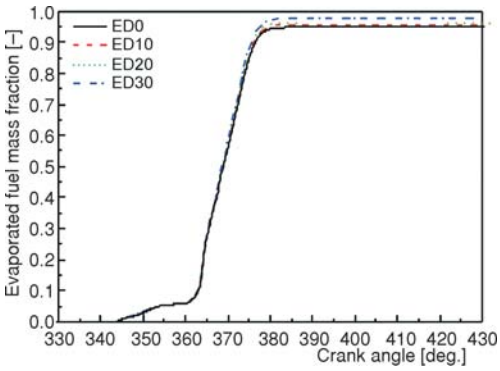

Figure 8. Evaporated fuel mass fractions

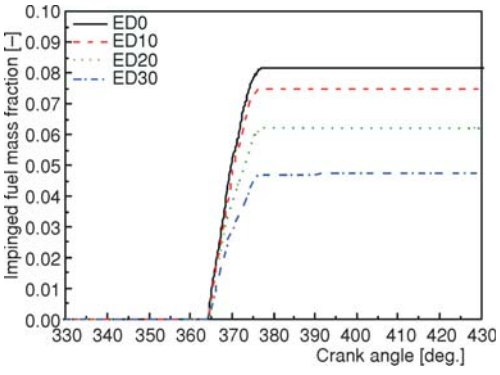

Figure 9. Impinged fuel mass fractions

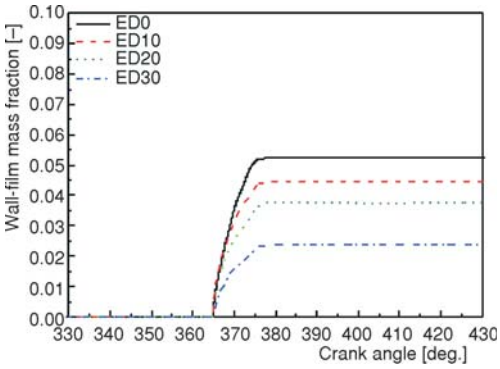

Figure 10. Wall-film mass fractions

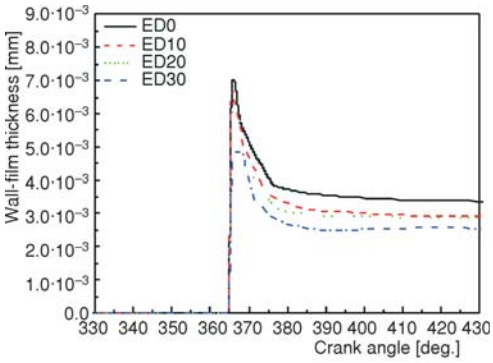

Figure 11. Wall-film thickness

In the pilot injection period, there is almost no fuel impinging into the combustion chamber. Furthermore, there is also no wall-film forming. The wall-films begin forming until the main injection starts. With the ethanol volume percentage increasing, the K' of blend fuels increase significantly, as reported in fig. 7. Thus the mass and thickness of the wall-film decrease with the increased ethanol volume percentage, as reported in figs. 10 and 11.

Effects of ethanol volume percentage on the combustion process

As ED0 has higher cetane number (reported in tab. 2), and less ignition delay period, it has earlier premixed combustion and higher rate of heat release than the blend fuels in the range from 350° CA to 357° CA. It is also found that the low heat values, the accumulated heat releases and the peak cylinder pressures of the blend fuels decrease with the increased ethanol volume percentage, as shown in figs. 12 and 13.

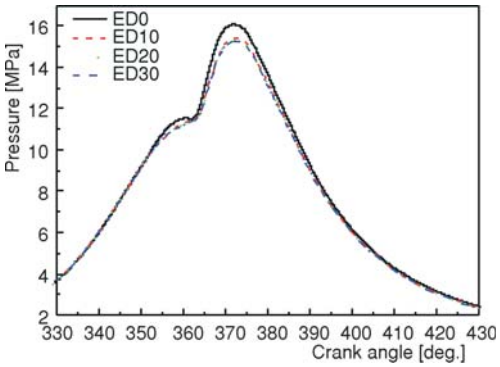

Figure 12. Cylinder pressure

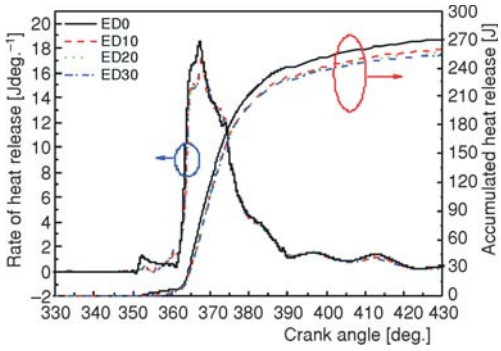

Figure 13. Rate of heat release and accumulated heat release

Effects of ethanol volume percentage on the exhaust emissions

The key region for NO_x formation is where the local temperature is higher than 1800 K [28], which is defined as the high temperature region. In order to couple the key region to investigate the effects of the ethanol volume percentage on the NO_x forming process, some codes are added into the Output control of the FIRE software, which could output the total mass of the high temperature region, and show the results in the 2-D results of the FIRE software. The codes

are just employed for outputting, which don't change the kinetic mechanism of the NO_x formation. The NO_x formation region mass fraction is the value of dividing the total mass of the high temperature region by the mass of the whole mesh. The details of the codes are reported in tab. 3.

Table 3. Codes for key region mass of NO_x and soot formation

Codes for the key region mass of NO_x formation	Codes for the key region mass of soot formation

double mass_ high temperature region;
if(init)
mass_NO_x = 0.0;
else
sum = mass_NO_x;
if(temp >= 1800) mass_NO_x +=
= den·vol;
return 0.0;
	double mass_rich fuel region;
	if(init)
	mass_rich fuel region = 0.0;
	else
	sum = mass_rich fuel region;
	double eps = 1.0e-10;
	double mass = den·vol;
	double egr_mf = YEGRMF[index];
	double fmixc = YFMIXC[index];
	double fo2e = (1.0-egr_mf)·FO2 + egr_mf·EGRCMP[1];
	double eqr = STO2/(fo2e+eps)·fmixc/(1.0-fmixc+eps);
	if(temp >1500 &&eqr > 1.5) mass_rich fuel region += den·vol;
	return 0.0;

Furthermore, the key region for soot formation is where the local equivalence ratio is bigger than 1.5 and temperature higher than 1500 K [29], which is defined as the rich fuel region. The similar codes are added into the Output control of the FIRE software. Meanwhile the codes are just employed for outputting, which do not change the kinetic mechanism of the soot formation. The soot formation region mass fraction is the value of dividing the total mass of the rich fuel region by the mass of the whole mesh. The codes are reported in tab. 3.

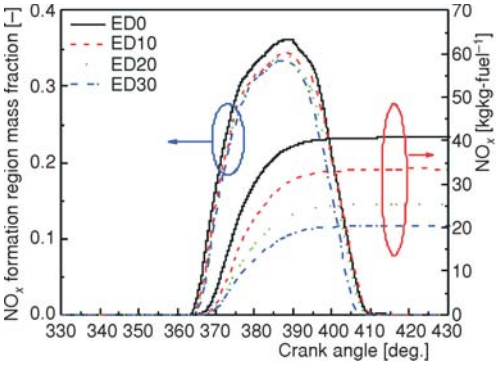

Figure 14. NO_x formation region mass fraction and NO_x emissions

From 360° CA (shown in fig. 13), the accumulated heat releases of the blend fuels begin releasing. Some regions in the cylinder become to high temperature region. Thus NO_x formation region mass fractions of the blend fuels become larger as reported in fig. 14. Almost at the same time, NO_x emissions begin increasing as shown in the right side of fig. 14. At 385° CA, NO_x formation region mass fractions come to the peak, while NO_x emissions also reach the highest point. With the increased ethanol volume percentage, the NO_x formation region mass fraction and NO_x emissions have the same changing trend – decreasing. It means that the NO_x formation region mass fraction displays a

good correlation with the NO_x formation. Coupled with the NO_x formation region mass fraction, it is easy and clear to understand the mechanism of NO_x formation.

As shown in fig. 2, huge fuels are injected into the cylinder from 365° CA, the rich fuel regions increase, causing the soot formation region mass fraction and the soot emissions becoming larger. At 375° CA, soot formation region mass fractions reach the highest point, as reported in fig. 15. The soot emissions also come to the peak. After 375° CA, the piston moves to bottom dead center (BDC), cylinder temperature decreases, while the rich fuel region and the soot formation region mass fraction decreases. With the increased ethanol volume percentage, the soot formation region mass fraction and the soot emissions have the same changing trend – decreasing. It implies that the soot formation region mass fraction displays a good correlation with the soot formation.

As shown in fig. 13, the ethanol-diesel blend fuels have less heat release from 350° CA to 357° CA. Moreover it affects the oxidation of CO, which occurs at least 1500 K [30]. As shown in fig. 16 (from 360° CA to 370° CA) and fig. 17 (for the column of 365° CA and 370° CA), the CO emissions of ethanol-diesel blend fuels are higher than that of diesel fuel. But after 375° CA, the good volatility and high

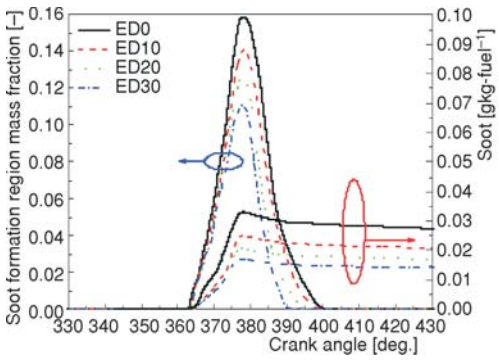

Figure 15. Soot formation region mass fraction and soot emissions

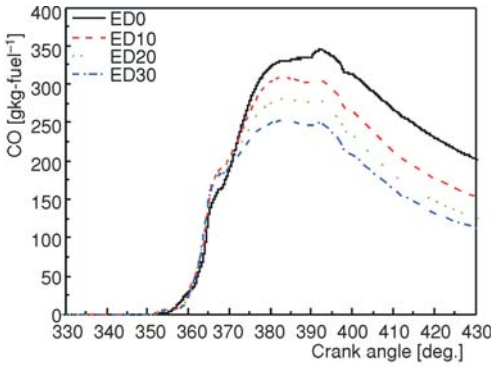

Figure 16. CO emissions

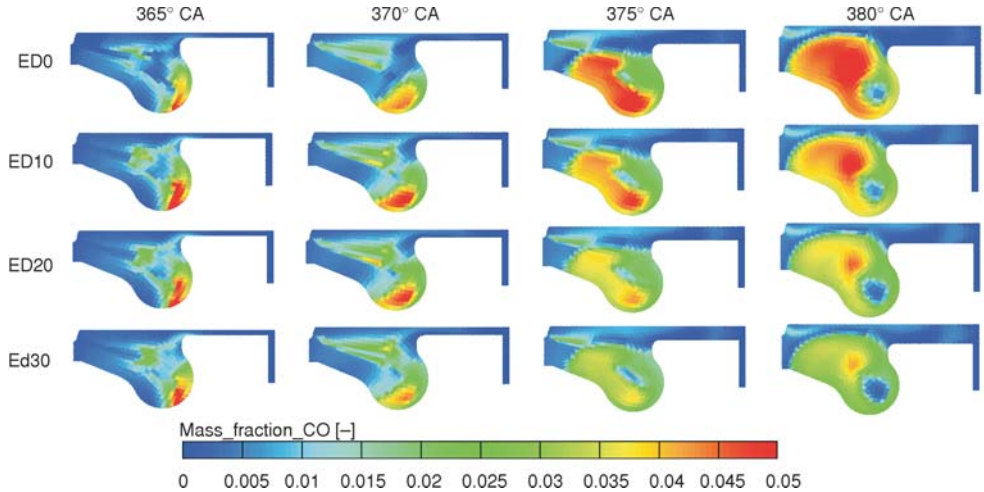

Figure 17. Contours for CO mass fraction (for color image see journal web site)

oxygen concentration of ethanol accelerates the atomized process of the blend fuels and increases the local air fuel ratio, which helps to decrease the CO emissions. So with the increased ethanol volume percentage, the CO emissions decrease, as shown in fig. 16 (from 375° CA to 430° CA) and fig. 17 (for the column of 375° CA and 380° CA).

Effects of ethanol volume percentage on the power output, economy and combustion noise

The power output of engine is evaluated by the indicated mean efficient power (IMEP). Due to the different low heat values of the blend fuels, the indicated specific fuel consumption (ISFC) is useless for evaluating the economy of engine. Equivalent indicated specific fuel consumption (EISFC) is defined here, which integrates the fuel energy to analyze the energy utilization:

$$EISFC = \frac{B_{\mathrm{ISFC}} H_{\mathrm{L}}}{H_{\mathrm{LD}}} \tag{10}$$

where H_{LD} is the low heat value of diesel and H_{L} – the low heat value of the blend fuel, calculated by mass percentage:

$$H_{\mathrm{L}} = \frac{(100 - ED)\rho_{\mathrm{D}} H_{\mathrm{LD}} + ED\rho_{\mathrm{E}} H_{\mathrm{LE}}}{(100 - ED)\rho_{\mathrm{D}} + ED\rho_{\mathrm{E}}} \tag{11}$$

The combustion noise is evaluated by ringing intensity RI [MWm^{-2}], which is developed by Eng [31, 32].

$$RI = \frac{\left[0.05\left(\frac{\mathrm{d}P}{\mathrm{d}t}\right)_{\max}\right]^2 \sqrt{399.9 T_{\max}}}{2.7 P_{\max}} \tag{12}$$

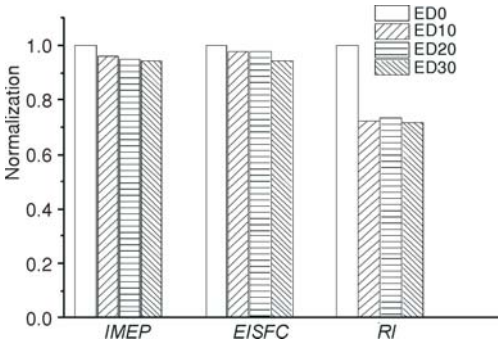

Figure 18. Normalized values of the *IMEP*, *EISFC* and *RI*

$(\mathrm{d}P/\mathrm{d}t)_{\max}$ [kPa/m] is the maximum rate of cylinder pressure rise, $T_{\max}$ [K] – the peak cylinder gas temperature; $P_{\max}$ [kPa] – the maximum cylinder pressure.

The *IMEP*, *EISFC* and *RI* are normalized, by the value of ED0. The results are reported in fig. 18. Due to the lower heat release and the cylinder pressure, the IMEP decreases with the increased ethanol volume percentage. The EISFC reduces with the increased ethanol volume percentage, which means that the energy utilizations of the blend fuels are not vitiated by ethanol. It is reported that $(\mathrm{d}P/\mathrm{d}t)_{\max}$ and $_{\mathrm{Pmax}}$ decrease with the increased ethanol volume percentage in fig. 12. Therefore the RI of the blend fuels also decrease with the increased ethanol volume percentage. It means that combustion noise of the blend fuels reduce with the increased ethanol volume percentage.

Conclusions

Based on the FIRE software to simulate atomization, wall-film formation and combustion process of ethanol-diesel blend fuels, and with the help of the codes adding to the FIRE soft-

ware to output the key region mass fraction for the NO_x and soot formation respectively, the conclusions of this study are:

- With the increased ethanol volume percentage, the evaporated fuel mass fractions increase, while impinged fuel mass fractions and wall-film mass fractions decrease.
- The blend fuels have longer ignition delay period. The total heat releases and cylinder pressures of the blend fuels decrease with the increased ethanol volume percentage, due to the lower low heat values.
- The NO_x and soot formation region mass fractions display a good correlation with the NO_x and soot formation. With the increased ethanol volume percentage, the NO_x and soot emissions decrease. The CO emissions decrease with the increased ethanol volume percentage, owing to the increased local air fuel ratio and the accelerated atomized process.
- The power output of engine penalize, while energy utilization of the blend fuel improve and combustion noise reduce, due to the increased ethanol volume percentage.

Acknowledgments

This work has been supported by the National Natural Science Foundation (No. 51006075) and the Shanghai municipal key subject construction project (B303). The authors gratefully acknowledge for the automobile engineering institute of Zhejiang Geely Holding Group Co. Thank them for providing the parameters of the HSDI diesel engine and the experimental results.

Nomenclature

Oh – Ohnesorge number
Re – Reynolds number

Greek symbols

ζ – velocity scale ratio, [–]
μ – viscosity, [mPs]
ρ – density, [kgm^{-3}]
σ – surface tension, [mNm^{-1}]

Acronyms

BDC – bottom dead center
ECFM – extended coherent flame model
ED – ethanol-diesel blend fuels
EISFC – equivalent indicated specific fuel consumption
IMEP – indicated mean efficient power
ISFC – indicated specific fuel consumption

References

[1] Ehleskog, R., *et al*., Effects of Multiple Injections on Engine-Out Emission Levels Including Particulate Mass from an HSDI Diesel Engine, SAE paper 2007-01-0910, 2007
[2] Cloudt, R., *et al*., Cost and Fuel Efficient SCR-Only Solution for Post-2010 HD Emission Standards, SAE paper 2009-01-0915, 2009
[3] Piscaglia, F., *et al*., Development of a CFD Model to Study the Hydrodynamic Characteristics and the Soot Deposition Mechanism on the Porous Wall of a Diesel Particulate Filter, SAE paper 2005-01-0963, 2005
[4] Rakopoulos, D. C., *et al*., Effects of Butanol-Diesel Fuel Blends on the Performance and Emissions of a High-Speed DI Diesel Engine, *Energy Conversion and Management, 51* (2010), 10, pp. 1989-1997
[5] Arul Mozhi Selvan, V., *et al*., Combustion Characteristics of Diesohol Using Biodiesel as an Additive in a Direct Injection Compression Ignition Engine under Various Compression Ratios, *Energy Fuels, 23* (2009), 11, pp. 5413-5422
[6] Çetin, M., *et al.*, Emission Characteristics of a Converted Diesel Engine Using Ethanol as Fuel, *Energy for Sustainable Development, 13* (2009), 4,pp. 250-554
[7] Corkwell, K. C., *et al*., Review of Exhaust Emissions of Compression Ignition Engines Operating on E Diesel Fuel Blends, SAE paper 2003-01-3283, 2003
[8] Naber, J. D., Farrell, P. V., Hydrodynamics of Droplet Impingement on a Heated Surface, SAE paper 930919, 1993
[9] Kalantari, D., Tropea, C., Spray Impact onto Flat and Rigid Walls: Empirical Characterization and Modeling, *International Journal of Multiphase Flow, 33* (2007), 5, pp. 525-544

[10] Yu, J., *et al*., The Study of Diesel Spray/Wall Impinging Process, *Transactions of CSICE, 21* (2003), 3, pp. 193-200
[11] Durbin, P.A., Near-Wall Turbulence Closure Modeling without Damping Functions, *Theor. Comput. Fluid Dyn., 3* (1991), 1, pp. 1-13
[12] Durbin, P. A., On the k-ε Stagnation Point Anomaly, *Int. J. Heat Fluid Flow, 17* (1996), 1, pp. 89-90
[13] Su, H., FIRE Solver Setup, AVL Report, 2006.8.31
[14] Speziale, C. G., *et al*., Modeling the Pressure-Strain Correlation of Turbulence: an Invariant System Dynamic Approach, *J. Fluid. Mech., 227* (1991), 2, pp. 245-272
[15] Hanjalic, K., *et al*., A Robust Near-Wall Elliptic-Relaxation Eddy-Viscosity Turbulence Model for CFD, *International Journal of Heat and Fluid Flow, 25* (2004), 6, pp. 1047-1051
[16] ***, AVL List GMBH, FIRE Manual, AVL List GMBH, 2008
[17] Brenn, G., *et al*., Computations and Experiments on the Evaporation of Multi-Component Droplets, *Proceedings*, 9th Int. Conf. Liquid Atomiz. Spray Syst. (ICLASS), Sorrento, Italy, 2003, pp. 5073-5086
[18] Shi., Li, G., Numerical Simulation of Combustion Process for DI Diesel Engine Based on Coherent Flame Model, *Vehicle Engine, 170* (2007), 4, pp. 31-36
[19] Zeldovich, Y. B., *et al*., Oxidation of Nitrogen in Combustion (translation by M. Shelef), Academy of Sciences of USSR, Institute of Chemical Physics, Moscow-Leningrad, 1947
[20] Tesner, P.A., *et al.*, Kinetics of Dispersed Carbon Formation, *Combustion and Flame, 17* (1971), 2, pp. 253-260
[21] Hiroyasu, H., Nishida, K., Simplified Three Dimensional Modeling of Mixture Formation and Combustion in a DI Diesel Engine, SAE paper 890269, 1989
[22] Bai, C., Gosman, A. D., Development of Methodology for Spray Impingement Simulation, SAE paper 950283, 1995
[23] Mundo, C., *et al.*, Droplet-Wall Collisions: Experimental Studies of the Deformation and Breakup Process, *Int. J. Multiphase Flow, 21* (1995), 2, pp. 151-173
[24] Mundo, C., *et al*. , Experimental Studies of the Deposition and Splashing of Small Liquid Droplets Impinging on a Flat Surface, ICLASS-94, Rouen, France, 1994, paper 1-18
[25] Jiao, Y., *et al.*, Multi-Dimensional Simulation of Effect of Combustion Chamber Geometry on Emission in DI Diesel Engine, *Chinese Internal Combustion Engine Engineering, 28* (2007), 4, pp. 11-15
[26] Bianchi, G. M., *et al*., Numerical Analysis of Passenger Car HSDI Diesel Engines With the 2nd Generation of Common-Rail Injection Systems: The Effects of Multiple Injections on Eissions, SAE paper 2001-01-1068, 2001
[27] Maiboom, A., *et al*., Experimental Study of Various Effects of Exhaust Gas Recirculation (EGR) on Combustion and Emissions of an Automotive Direct Injection Diesel Engine, *Energy, 33* (2008), 1, pp. 22-34
[28] Jin Hua-Yu, Effects of Key Initial Boundaries on the Combustion of Diesel Engine and Their Optimization Strategies, Ph. D. thesis, Jilin University, Jillin, China, 2008
[29] Arcoumanis, C., Schindler, K.-P., Mixture Formation and Combustion in the DI Diesel Engine, SAE paper 972681, 1997
[30] Huang, H.-Z, *et al*., Study of the Effects of Mixing on Low-temperature Diesel Combustion Based on CO-Φ-T Map, *Transactions of CSICE, 27* (2009), 2, pp. 97-102
[31] Eng, J. A. Characterization of Pressure Waves in HCCI Combustion, SAE paper 2002-01-2859, 2002
[32] Siewert, R. M., Spray Angle and Rail Pressure Study for Low NO_x Diesel Combustion, SAE paper 2007-01-0122, 2007

Paper submitted: October 7, 2011
Paper revised: April 18, 2012
Paper accepted: May 29, 2012